Polymer 51 (2010) 4200–4210

Contents lists available at ScienceDirect

Polymer

journal homepage: www.elsevier.com/locate/polymer

Synthesis, characterization and biodegradation of poly(ester amide)s based hydrogels

Xuan Pang [a,1], Chih-Chang Chu [a,b,*]

[a] Department of Fiber Science and Apparel Design, Cornell University, Ithaca, NY 14853-4401, USA
[b] Biomedical Engineering Program, Cornell University, Ithaca, NY 14853-4401, USA

ARTICLE INFO

Article history:
Received 25 April 2010
Received in revised form
3 July 2010
Accepted 10 July 2010
Available online 17 July 2010

Keywords:
Poly(ester amide)s
Biodegradation
Hydrogel

ABSTRACT

A series of new biodegradable hybrid hydrogels were designed and fabricated from a new family of amino acid-based functional poly(ester amide) (**PEA-AG**) and commercial poly(ethylene glycol) diacrylate (**PEG-DA**) or Pluronic diacrylate (**Pluronic-DA**) by UV photocrosslinking. These biodegradable hybrid hydrogels were characterized in terms of equilibrium swelling ratio (Q_{eq}), compression modulus by dynamic mechanical analysis (DMA), and interior morphology by scanning electron microscope (SEM). Both the precursors' chemical structures and feed ratio had significant effect on the properties of the hybrid hydrogels. All these hybrid hydrogels had a three-dimensional porous network structure. The hydrophobicity, crosslinking density and mechanical strength of the hybrid hydrogels increased with an increase in allylglycine (**AG**) content in the PEA-AG, but the swelling and pore size of the hybrid hydrogels decreased. The biodegradation rate of these hybrid hydrogels in an enzyme (α-chymotrypsin) solution was faster than in a pure PBS buffer control, and the biodegradation rate increased with an increase in α-chymotrypsin concentration and allylglycine content.

1. Introduction

Hydrogels have attracted significant attentions for their use as medical implants, diagnostics, biosensors, bioreactors, bioseparators, and matrices for drug delivery and tissue engineering because hydrogels have high water contents like body tissues and are highly biocompatible [1]. Hydrogels could be broadly divided into two categories: non-biodegradable and biodegradable. The biodegradable hydrogels are more useful in biomedical field because they are fabricated from biodegradable polymer-based precursors [2–11], and do not have permanent foreign-body response inside human body. Biodegradable polymers based hydrogels as drug carriers have become increasingly important because they can not only be degraded and eliminated from the body after use but also provide flexibility in the design of delivery devices for large molecular weight drugs, such as pharmaceutically active proteins and polypeptides.

Amino acid-based poly(ester amide) (**PEAs**) which are prepared from amino acids, fatty alcohols and acids and have both ester and amide blocks on their backbones, have been introduced as new biodegradable biomaterials [12–25]. These PEAs integrate good mechanical, thermal and processing properties of polyamides and the biodegradability of polyesters into a single entity [23,26]. These PEAs have shown very unique and promising biological characteristics, such as very low level of inflammation, promoting endothelial cell attachment and proliferation, as well as blood biocompatibility [12,24,25]. These amino acid-based PEAs have also been fabricated into a wide range of physical forms like drug-eluting electrospun fibrous membranes [27,28], 3D microporous hydrogel drug carriers [29], drug-eluting microspheres [27] and nanoparticles as transfection agents [30].

Most of the published amino acid-based PEAs have used saturated fatty alcohols/acids, and hence the resulting PEAs are saturated PEAs. Recently, Kai et al. reported unsaturated PEAs (UPEA) synthesized from unsaturated fatty alcohols/acids [13,15,17,18,20]. These UPEAs have carbon–carbon double bonds in the PEA backbone, and were used as precursors to fabricate PEA-based hydrogels via photocrosslinking [17,20,29].

We have very recently, developed an alternative to synthesize unsaturated PEAs (**PEA-AG**). Instead of using unsaturated fatty alcohols/acids to provide double bonds in the PEA backbones, this alternative uses an amino acid derivative, DL-2-allylglycine (**AG**), to provide pendant carbon–carbon double bonds to PEAs, and hence the resulting unsaturated PEA-AG have reactive pendant double bonds [31]. The contents of the pendant double bond in these new

* Corresponding author. Department of Fiber Science and Apparel Design, Cornell University, Ithaca, NY 14853-4401, USA. Tel.: +1 607 255 1938; fax: +1 607 255 1093.
E-mail address: cc62@cornell.edu (C.-C. Chu).
[1] Current address: Chinese Academy of Science, Institute of Applied Chemistry, 5625 Renmin Street, Changchun, Jinlin 130022, China.

0032-3861/$ – see front matter © 2010 Published by Elsevier Ltd.
doi:10.1016/j.polymer.2010.07.015

unsaturated PEA-AGs were tunable by adjusting the feed ratio of AG to another regular amino acid like L-phenylalanine (**Phe**). The reactivity of the pendant double bonds in the AG unit was demonstrated by synthesizing new functional PEA-AG derivatives from the PEA-AG.

The aim of this work is to further demonstrate the feasibility of the formation of a series of new biodegradable hybrid hydrogels through the photo-crosslinkable pendant carbon–carbon double bonds in the PEA-AGs with other non-PEA precursors like poly (ethylene glycol) diacrylate (**PEG-DA**) or pluronic diacrylate (**Pluronic-DA**). The resulting hybrid hydrogels were characterized by their gel fraction (G_f), equilibrium swelling ratio (Q_{eq}), compressive modulus, and interior morphology. The effects of the precursor feed ratio (PEA-AG to PEG-DA) on the property of the hybrid hydrogels were studied. The biodegradation of these hybrid hydrogels having different precursors' feed ratios were also examined in both pure PBS buffer and α-chymotrypsin solution. The weight loss and the interior morphology change of hydrogels were monitored during the whole degradation period.

2. Experimental section

2.1. Materials

DL-2-Allylglycine (**AG**), L-Phenylalanine (**Phe**), *p*-toluenesulfonic acid monohydrate (TosOH·H_2O), hydroquinone, sebacoyl chloride, succinyl chloride, 1,4-butanediol, 1,6-hexanediol (Alfa Aesar, Ward Hill, MA) and *p*-nitrophenol (J. T. Baker, Phillipsburg, NJ) were used without further purification. Triethylamine from Fisher Scientific (Fairlawn, NJ) was dried via refluxing with calcium hydride and then distilled. Other solvents, such as benzene, ethyl acetate, acetone, *N,N*-dimethylacetamide (DMA) and dimethyl sulfoxide (DMSO), were purchased from VWR Scientific (West Chester, PA) and were purified by standard methods before use. PEG-DA (PEG $M_n = 4000$), Pluronic-DA (Pluronic F68 $M_n = 7000$) were synthesized in our group as described previously [20,32].

2.2. Synthesis of the PEA-AG polymers

PEA-AG having pendant carbon–carbon double bonds were prepared through the solution co-polycondensation of di-*p*-nitrophenyl ester with a mixture of di-*p*-toluenesulfonic acid salts of bis-L-phenylalanine and bis-DL-2-allylglycine esters in a pre-determined mixture ratio [17,31]. The combinations used in this work were listed in Table 1 and illustrated in Fig. 1.

2.3. Preparation of PEA-AG based hybrid hydrogels PEA-AG-G

PEA-AG-G biodegradable hydrogels (PEA-AG-G_{PEG} or PEA-AG-$G_{Pluronic}$) were prepared by the photocrosslinking of PEA-AG with PEG-DA or Pluronic-DA precursors. Irgacure 2959® was used as a photo-initiator. The PEA-AG itself, however, could not form gels via photocrosslinking.

An example of the fabrication method for such a hybrid hydrogel (8-Phe-4-AG-4-G_{PEG}) from 8-Phe-4-AG-4 and PEG-DA precursors was given below. A weight ratio of 1–3 of 8-Phe-4-AG-4 to PEG-DA (0.08 g of 8-Phe-4-AG-4 and 0.24 g of PEG-DA) was added to a vial and dissolved in 2 mL of DMA to form a clear, homogeneous solution with a light yellow color. The photo-initiator Irgacure 2959® (0.016 g, 5 wt.% of the total amount of the precursors) was added to the solution and dissolved completely at room temperature. The solution was irradiated by a long-wavelength UV lamp (365 nm, 100 W) for 15 min in a Teflon mold at room temperature and gel formation occurred.

The resultant hydrogel (diameter 25 mm, thickness 4 mm) was removed carefully from the mold and washed with distilled water to remove any residual chemicals. The distilled water was replaced periodically. After this purification process, the hydrogels was soaked in distilled water until swelling equilibrium and then removed and dried in vacuo at room temperature for 48 h before the following characterization. The gelation efficiency, G_f, was used to describe the capability of hydrogel formation through the following equation:

$$G_f = \frac{W_d}{W_p} \times 100\% \quad (1)$$

where W_d is the weight of the dry hydrogel and W_p is the total feed weight of the two macromer precursors and the photo-initiator.

Table 1
List of monomers and functional PEA-AGs synthesized by different monomer combinations.

Monomer I		Monomer II	Polymer	
AG-6	Phe-4	N-2	2-Phe-4-AG-6	2-Phe-6-AG-6
	Phe-6	N-8	8-Phe-4-AG-6	8-Phe-6-AG-6
AG-4	Phe-4	N-2	2-Phe-4-AG-4	2-Phe-6-AG-4
	Phe-6	N-8	8-Phe-4-AG-4	8-Phe-6-AG-4

2.4. Interior morphology of hydrogles

Scanning electron microscopy (SEM) was employed to analyze the interior morphological structure of the PEA-AG hydrogels as a function of the precursor feed ratio. A cryofixation technique was used to observe the swollen hydrogel structure with minimal artifacts. Typically, an individual hydrogel was incubated in distilled water at room temperature for 3 days to reach its equilibrium swelling. The hydrogel was then gently removed and immediately transferred into liquid nitrogen to freeze and retain the swollen structure. The sample was subsequently freeze-dried for 72 h in a Virtis (Gardiner, NY) freeze drier in vacuo at −40 °C and finally fixed on aluminum stubs and coated with gold for 60 s for SEM observation with a Hitachi (Mountain View, CA) S4500 SEM instrument. Image analyses of SEM photographs were performed by using the public domain NIH Image program (http://rsb.info.nih.gov/nih-image/).

2.5. Swelling kinetics

The swelling kinetics of the PEA-AG-G hydrogels was measured over a period of 7 days at room temperature. Dry PEA-AG-G hydrogels were weighed and immersed in 15 mL of distilled water at room temperature for pre-determined periods; they were then removed, and surface water was blotted by the filter paper and weighed until there was no further weight change. The swelling ratio (Q) was calculated as follows:

$$Q = \frac{W_s - W_d}{W_d} \times 100\% \quad (2)$$

where W_s is the weight of the swollen hydrogel at time t and W_d is the weight of the dry hydrogel at $t = 0$.

2.6. Mechanical testing

The mechanical testing of the PEA-AG-G hydrogels was performed on a DMA Q800 Dynamic Mechanical Analyzer (TA Instruments Inc., New Castle, DE) in a "controlled force" mode. The swollen hydrogel samples in circular disc shape were submerged in distilled water and mounted between the movable compression

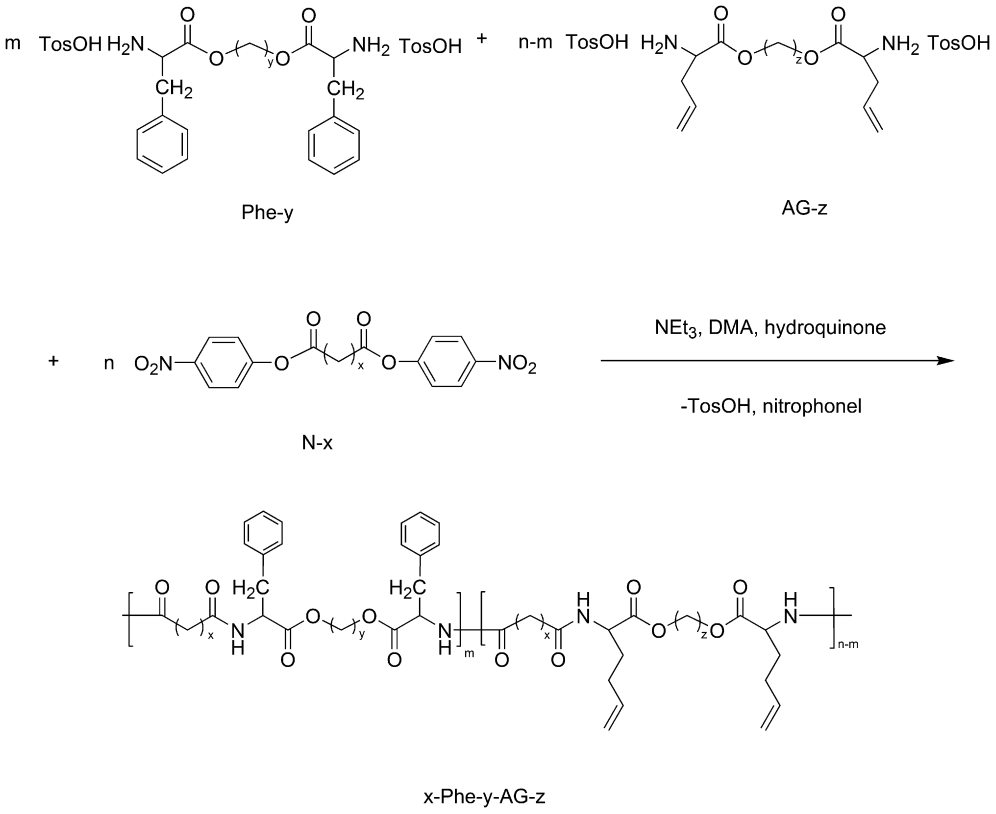

Fig. 1. Synthetic pathway for the preparation of functional poly(ester amide)s having pendant carbon–carbon double bonds.

probe (diameter 15 mm) and the fluid cup. A compression force from 0.01 to 0.05 or 0.30 N (depending on the gel strength) at a rate of 0.02 or 0.05 N/min was applied at room temperature. The compression elastic modulus (E) of the swollen hydrogel was extracted by plotting the compressional force versus strain [17].

2.7. In vitro enzymatic biodegradation of PEA-AG hybrid hydrogels PEA-AG-G_{PEG}

The biodegradation of PEA-AG/PEG-DA hybrid hydrogels PEA-AG-G_{PEG} was carried out in a small vial containing a small piece of dry hydrogel sample (ca. 80 mg) and 10 mL of PBS buffer (pH 7.4, 0.1 M) with α-chymotrypsin at different concentrations (0.1 or 0.2 mg/mL). Pure PBS buffer was used as a control. The vial was then incubated at 37 °C with a constant reciprocal shaking (100 rpm). The incubation media were refreshed daily in order to maintain enzymatic activity. At pre-determined immersion durations, hydrogel samples were removed from the incubation medium; washed gently with distilled water, and then lyophilized in vacuo with FreeZone Benchtop and Console Freeze Dry System (Model 7750000, LABCONCO Co., Kansas City, MO) at −40 °C for 72 h to a constant weight. The degree of biodegradation was estimated from the weight loss of the hydrogel based on the following equation:

$$W_l(\%) = \frac{W_o - W_t}{W_o} \times 100 \quad (3)$$

where W_o was the original weight of the dry PEA-AG-G hydrogel sample before immersion, and W_t was the dry PEA-AG-G hydrogel sample weight after incubation for t days (with or without the enzyme). The weight loss averaged for three specimens was recorded.

3. Results and discussions

3.1. PEA-AG-G hydrogels formulation

In order to investigate the potential applications of the newly synthesized functional PEA-AG in biomedical and pharmaceutical fields, 8-Phe-4-AG-4 was used as a representative PEA-AG precursor to fabricate hybrid hydrogels with PEG-DA or Pluronic-DA co-precursor by UV irradiation. Optical image of a representative PEA-AG/PEG-DA and PEG-AG/Pluronic-DA hybrid hydrogels was shown in Fig. 2. A representative network structure of these hybrid hydrogels was shown in Fig. 3.

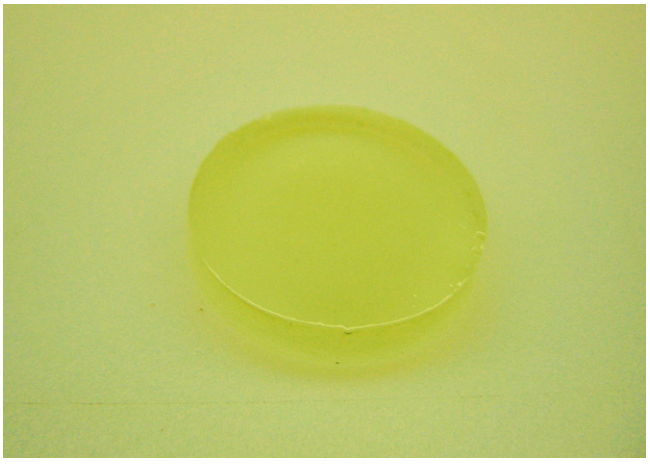

Fig. 2. Optical image of hybrid hydrogels 8-Phe-4-AG-4-25-G_{PEG}.

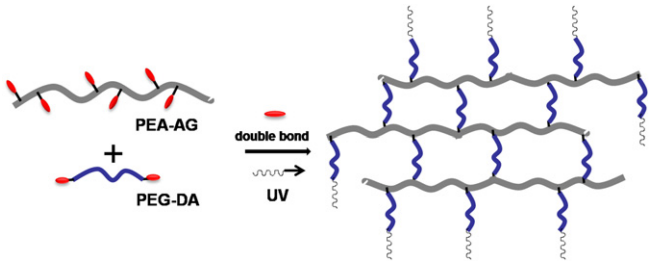

Fig. 3. One of the possible photo-crosslinked structures between PEA-AG and PEG-DA.

The FTIR spectra of a typical PEA-AG-GPEG hydrogel, 8-Phe-4-AG-4-25-GPEG, and its precursors, 8-Phe-4-AG-4-25 and PEG-DA, were shown in Fig. 4. The characteristic absorption bands of the unsaturated = CH stretch from the AG unit (~ 3030 cm^{-1}) in 8-Phe-4-AG-4-25, and the unsaturated ester C=O bond (acrylate, ~ 1722 cm^{-1}) in PEG-DA disappeared in the 8-Phe-4-AG-4-25-GPEG hydrogel. This was because the carbon–carbon double bonds were consumed during the UV photocrosslinking reactions. Meanwhile, the characteristic absorption peaks of the normal (saturated) ester group (~ 1736 cm cm^{-1}) and amide group (~ 1649 and ~ 1536 cm^{-1}) from 8-Phe-4-AG-4-25 and ether groups (~ 1114 cm^{-1}) from PEG-DA appeared in the IR spectra of the FPBe-G28 hydrogel, and they also suggested the coupling of the two precursors.

In our previously reported UPEA hydrogel systems [17,20], the photo-crosslinkable double bond in the UPEA precursor was imbedded in the UPEA backbone, and the double bond contents could only be controlled by the molecular weight of the UPEA. The new PEA-AG-based hydrogel system reported here, however, had the advantage that the double bond was pendant and their contents were adjustable by controlling the Phe to AG feed ratio in the synthesis of the x-Phe-y-Ag-z precursor; therefore, the cross-linking level of the PEA-AG-based hydrogels could be tailored by tuning the feed ratio of the two amino acids in the x-Phe-y-Ag-z precursors, i.e., Phe-y to AG-z.

The PEA-AG-based hydrogels fabricated had the character of amphiphilic nature because they consist of both hydrophobic segments from the PEA-AG precursors and hydrophilic segments from either PEG-DA or Pluronic-DA precursors.

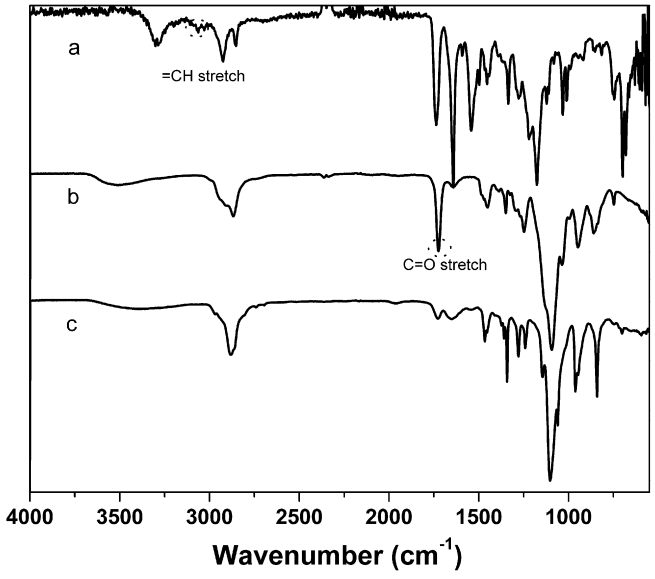

Fig. 4. FTIR spectra of (a) 8-Phe-4-AG-4-25, (b) PEG-DA and (c) 8-Phe-4-AG-4-25-G_{PEG}.

To evaluate the effect of the different types of PEA-AG precursor on the properties of the resulting hybrid hydrogels, a series of PEA-AGs of different Phe-4 to AG-4 mole ratios (3:1, 2:1, 1:1) were synthesized and used as the precursors to fabricate hybrid hydrogels with either PEG-DA or Pluronic-DA co-precursor at the constant weight feed ratio of PEA-AG to the co-precursor (1:3). The gelation efficiency, G_f, was found to increase with an increase in the AG-4 content in the PEA-AG precursor as shown in Table 2. For example, the G_f values of the 8-Phe-4-AG-4-G hydrogels increased from 84% of 8-Phe-4-AG-4-25-G_{PEG}, 88% of 8-Phe-4-AG-4-33-G_{PEG} to 94% of 8-Phe-4-AG-4-50-G_{PEG}. The higher G_f values manifested a higher conversion yield of the precursors, and therefore, a higher level of crosslinked hydrogel structure formed. This was because an increase in the AG-4 content in the PEA-AG precursor would result in a corresponding increase in the pendant double bonds located in the AG unit, i.e., more crosslinkable sites.

Comparing with the corresponding PEA-AG-G_{PEG} hydrogel, the PEA-AG-$G_{Pluronic}$ hydrogel had relatively lower G_f values. The relatively low G_f value was attributed to the low double bond density. For both PEG-DA (PEG M_n = 4000) and Pluronic-DA (Pluronic F68 M_n = 7000) precursors, polymer chains were end-capped with only two photo-crosslinkable double bonds, but the Pluronic-DA had a longer chain, and therefore, lower double bond density. When Pluronic-DA photo-crosslinked with the corresponding PEA-AG precursor, the hydrogels formed would have a relatively looser network structure.

3.2. Swelling of the hydrogels

The swelling property of all the hydrogels was investigated by the swelling kinetic studies in distilled water at room temperature. All the hydrogel samples swelled fast, and within 8 h they all reached 90% of their final equilibrium swelling weight (Q_{eq}), the swelling rates became significantly lower thereafter. The Q_{eq} values of the hybrid hydrogels were listed in Table 2. Both pure pluronic-DA and PEG-DA hydrogels had higher Q_{eq} values (1520 ± 40% and 1300 ± 50%) than the hybrid hydrogels. The effect of AG contents and the methylene chain length in the PEA-AG backbone on swelling was given below.

3.2.1. Effect of the allylglycine (AG) segment content on swelling

The Q_{eq} values of the hybrid hydrogels decreased with a decrease in the feed ratio of Phe-y to AG-z (i.e., increasing AG content) in the PEA-AG precursor. For example, the 8-Phe-4-AG-4-25-G_{PEG} hydrogel had the Q_{eq} value of 860 ± 20% as the Phe-4:AG-4 ratio was 3:1, while the 8-Phe-4-AG-4-50-G_{PEG} hydrogel at the Phe-4:AG-4 ratio 1:1 had half of the Q_{eq} value of 8-Phe-4-AG-4-25-G_{PEG} (430 ± 30%, Fig. 5). Similar Q_{eq} were found in the 8-Phe-4-AG-4-25-$G_{pluronic}$

Table 2
Properties of PEA-AG-G Hydrogels.[a]

Sample	Mole feed ratio of Phe to AG	G_f (%)	Q_{eq} (× 100%)	Compressive modulus (MPa)
Pure PEG-DA	N/A	70	13.0 ± 0.5	0.066 ± 0.004
8-Phe-4-AG-4-25-G_{PEG}	3:1	84	8.6 ± 0.2	0.242 ± 0.071
8-Phe-4-AG-4-33-G_{PEG}	2:1	88	6.0 ± 0.3	0.351 ± 0.092
8-Phe-4-AG-4-50-G_{PEG}	1:1	94	4.3 ± 0.3	0.557 ± 0.105
2-Phe-4-AG-4-25-G_{PEG}	3:1	86	7.5 ± 0.2	0.290 ± 0.065
2-Phe-4-AG-4-50-G_{PEG}	1:1	95	4.0 ± 0.3	0.732 ± 0.097
Pure Pluronic-DA	N/A	61	15.2 ± 0.4	0.015 ± 0.003
8-Phe-4-AG-4-25-$G_{Pluronic}$	3:1	77	10.7 ± 0.1	0.165 ± 0.082
8-Phe-4-AG-4-33-$G_{Pluronic}$	2:1	82	7.8 ± 0.2	0.280 ± 0.078
8-Phe-4-AG-4-50-$G_{Pluronic}$	1:1	87	6.2 ± 0.3	0.442 ± 0.112
2-Phe-4-AG-4-25-$G_{Pluronic}$	3:1	78	10.0 ± 0.1	0.206 ± 0.096

[a] The weight ratio of PEA to PEG-DA and PEA to Pluronic-DA was kept as 1–3.

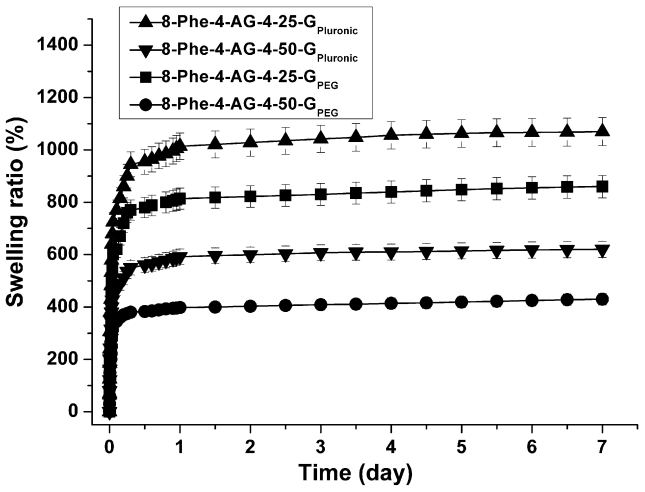

Fig. 5. Swelling behaviors of PEA-AG-G_{PEG} and PEA-AG-$G_{Pluronic}$ hydrogels with different allylglycine segment content.

hybrid hydrogels: 1070 ± 10% Q_{eq} at the Phe-4:AG-4 was 3:1, vs. 620 ± 30% Q_{eq} at the Phe-4:AG-4 ratio 1:1 (Fig. 5). As the Phe-y to AG-z feed ratio decreased, AG unit increased which resulted in higher pendant double bond contents, i.e., providing more crosslinkable sites for producing a tighter network structure and lower Q_{eq} value. This tighter gel network also led to a higher compressive modulus as described later. Comparing with the corresponding PEA-AG-G_{PEG} hydrogel, the PEA-AG-$G_{Pluronic}$ hydrogel had relatively higher Q_{eq} values due to the lower double bond density in Pluronic-DA precursor.

3.2.2. Effect of the methylene chain length in PEA-AG precursor on swelling

The effect of the methylene chain length in PEA-AG backbone on the swelling ratios of the PEA-AG-G hydrogels was shown in Fig. 6. At a constant PEA-AG to PEG-DA feed ratio (1:3), a shorter diacid $-CH_2-$ segment (i.e., x) from C_8 (8-Phe-4-AG-4-25-G_{PEG}) to C_2 (2-Phe-4-AG-4-25-G_{PEG}) decreased the Q_{eq} value slightly from 860 ± 20% to 750 ± 20%. This relationship between the shorter methylene chain length in PEA-AG precursor and lower hybrid hydrogel equilibrium swelling was attributed to the formation of a tighter network structure from denser double bond contents due to shorter methylene chain spacer between two adjacent double bonds. Similar trend was also found in the Pluronic series (Table 2).

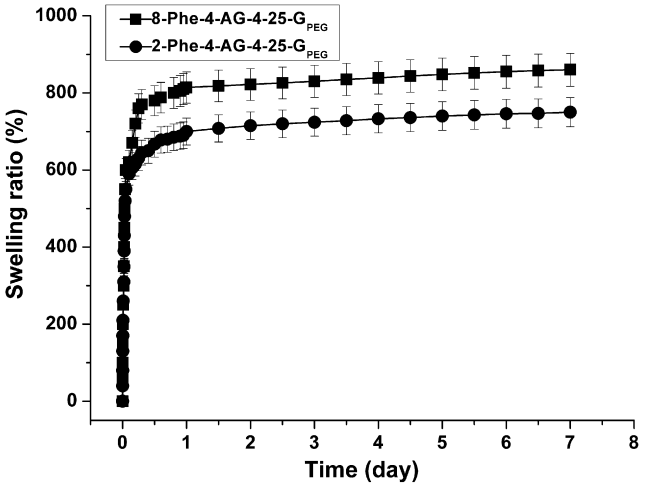

Fig. 6. Swelling behaviors of PEA-AG-G_{PEG} with different backbone length.

3.2.3. Effect of the double bond locations in PEA-AG on swelling

When hybridized with PEG-DA co-precursor, the location of the carbon–carbon double bonds in PEA precursor could have a profound different effect on the hydrogel properties. In our prior hydrogel research [20], the double bonds were introduced into the PEA backbone as unsaturated PEA (UPEA) precursor, the hydrogels formed had a wide range of Q_{eq} from 360 ± 20% to 920 ± 70%. And the double bond in the diamide portion of each repeating unit had a higher reactivity than the double bond in the diester portion. The higher reactivity of the double bonds in the diamide portion could be attributed to the conjugation interaction between the double bonds and the carbonyl group of the diamide in fumaryl-based UPEAs. The electro-withdrawing ability of the carbonyl carbon stabilized the free radicals formed during the polymerization and hence facilitated the attack on the double bond; that is, it was more reactive toward photocrosslinking. For example, the Q_{eq} value of hybrid hydrogels formed from 2-UPhe-4 (double bond in the diamide portion) with PEG-DA co-precursor was 360 ± 20%. While the corresponding hybrid hydrogels (same x and y) from PEA-AG and PEG-DA precursors was 400 ± 30% (2-Phe-4-AG-4-50-G_{PEG}). The Q_{eq} value of the corresponding PEA-AG-based hydrogels was lower than UPEA-based hydrogels. The only difference between PEA-AG and UPEA precursors was the double bonds location, where UPEA had the double bonds located in backbone, PEA-AG in side chain. Although in the UPEA-based hydrogel system, the molecular weight of PEG-DA (PEG $M_n = 8000$) was higher than those in PEA-AG-based system (PEG $M_n = 4000$), but the double bond in the PEA precursor was the main factor that affecting the hydrogel property. It was believed that the pendant double bonds in PEA-AG were more accessible than those backbone double bonds in UPEA. Considering the Q_{eq} data, it was suggested that the reactivity of the pendant double bonds in PEA-AG was lower than those UPEAs with double bonds in the diamide portion.

3.3. Mechanical properties of the hydrogels

The compressive moduli of the hybrid hydrogels along with the pure PEG-DA and Pluronic-DA hydrogel controls were listed in Table 2. All PEA-AG-based hybrid hydrogels had their compressive moduli significantly higher than both the pure PEG-DA (0.066 ± 0.004 MPa) and Pluronic-DA (0.015 ± 0.003 MPa) hydrogel controls. For example, 8-Phe-4-AG-4-50-G_{PEG} has its compressive modulus more than 8 times greater than the pure PEG-DA hydrogel, i.e., 0.557 ± 0.105 MPa vs. 0.066 ± 0.004 MPa. Similar trend was also found in the Pluronic series.

The compressive modulus data in Table 2 also showed that an increase in the AG contents in the PEA-AG precursor resulted in hybrid hydrogels having higher compressive moduli. For example, the compressive moduli of the series of hydrogels PEA-AG-G_{PEG} increased from 0.242 ± 0.071 MPa for 8-Phe-4-AG-4-25-G_{PEG} (Phe-4:AG-4 = 3:1), 0.351 ± 0.092 MPa for 8-Phe-4-AG-4-33-G_{PEG} (Phe-4:AG-4 = 2:1), to 0.557 ± 0.105 MPa for 8-Phe-4-AG-4-50-G_{PEG} (Phe-4:AG-4 = 1:1). Similar trend was observed in the Pluronic hydrogel series. These mechanical data were also consistent with the equilibrium swelling data Q_{eq} shown in Table 2 that a tighter network structure due to a higher AG content led to hybrid hydrogels having higher compressive moduli and lower equilibrium swelling.

The relatively lower compressive moduli of the pure PEG-DA and pure Pluronic-DA hydrogels were due to their relatively lower double bond contents. For both PEG-DA and Pluronic-DA, the polymer chains were end-capped with only two photo-

crosslinkable double bonds; therefore, the hydrogels formed had a loose network structure. The PEA-AG-based precursors, however, had far more photo-crosslinkable pendant double bonds along the PEA-AG, and could contribute to the formation of a tighter network structure of the hybrid hydrogels with the PEG-DA or Pluronic-DA co-precursor. The increase in AG-4 contents in PEA-AG precursors would result in tighter network structure, higher compressive moduli and lower equilibrium swelling.

Comparing with the corresponding PEA-AG-G_{PEG} hydrogel, the PEA-AG-$G_{Pluronic}$ hydrogel had relatively lower compressive moduli. Because Pluronic-DA had a longer chain, and lower double bond density, so the hydrogels formed would have a relatively looser network structure. This was also consistent with the observed equilibrium swelling data in Table 2.

When comparing with UPEA-based hydrogels [20], the hydrogels from PEA-AG family had relatively lower compressive moduli than those UPEA hydrogels having double bond in the diamide portions of the UPEA backbone (2-Phe-4-AG-4-50, 0.732 ± 0.097 MPa and 2-UPhe-4, 1.2 MPa). Because of the conjugation interaction between the double bonds and the carbonyl group of the diamide in fumaryl-based UPEAs, the double bonds in the diamide portion of the PEA backbone had higher reactivity than PEA-AG-based hydrogels. These mechanical data was also consistent with the equilibrium swelling data.

3.4. Interior morphology of hydrogels

The interior morphological structures of the PEA-AG-based hybrid hydrogels were investigated by scanning electron microscopy (SEM) systematically as a function of the AG contents and the methylene chain length in the PEA-AG precursor. All the hybrid hydrogels exhibited well-defined, irregular and three-dimensional porous network structures, and their images will be presented and discussed below as a function of precursors' feed ratios and methylene chain length in the PEA-AG precursor.

3.4.1. PEA-AG/PEG-DA hybrid hydrogels (PEA-AG-G_{PEG})

The SEM images of the PEA-AG/PEG-DA hybrid hydrogels (PEA-AG-G_{PEG}) and the pure PEG-DA hydrogel were showed in Fig. 7. When comparing with the pure PEG-DA hydrogel (Fig. 7a, average diameter 20.4 ± 4.0 μm), PEA-AG-G_{PEG} hydrogles had relatively smaller pore size, and this pore size reduction became larger when the AG contents in the PEA-AG precursor increased. For example, the 8-Phe-4-AG-4-25-G_{PEG} had the average pore size 13.8 ± 2.9 μm (Fig. 7b), while the 8-Phe-4-AG-4-33-G_{PEG} and 8-Phe-4-AG-4-50-G_{PEG} had pores 9.7 ± 1.9 μm (Fig. 7c), and 5.3 ± 1.5 μm, respectively (Fig. 7d).

The effect of the methylene chain length of PEA-AG precursors (i.e. x, y and z in the x-Phe-y-AG-z) on the interior morphology of PEA-AG-G_{PEG} hydrogels were shown in Fig. 8. The effect of x of the PEA-AG precursors (8-Phe-4-AG-4-25 vs. 2-Phe-4-AG-4-25) was showed in Fig. 8a and b. Comparing with the 8-Phe-4-AG-4-25-G_{PEG} (Fig. 8a, average diameter 13.8 ± 2.9 μm), 2-Phe-4-AG-4-25-G_{PEG} had slightly smaller pore size (Fig. 8b, average diameter 10.9 ± 4.5 μm). The only structural difference between these two functional PEA-AGs was the number of CH_2 groups in the diacid segment. Shortening the diacid backbone from C_8 to C_2 had little effect on the hydrogel pore size. The effect of y of the PEA-AG precursors (8-Phe-4-AG-4-25 vs. 8-Phe-6-AG-4-25) was shown in Fig. 8a and c. Similar porous network with similar average pore sizes were observed (Fig. 8c, 8-Phe-6-AG-4-25, average diameter 12.5 ± 3.9 μm). The effect of z of the PEA-AG precursors (8-Phe-4-AG-4-25 vs. 8-Phe-4-AG-6-25) was shown in Fig. 8a and d. A similar result as the x and y was found for z as lengthening the allylglycine-based diester backbone from C_4 to C_6 would have little effect on hydrogel pore size. (Fig. 8d, 8-Phe-4-AG-6-25-G_{PEG} average diameter 12.2 ± 2.9).

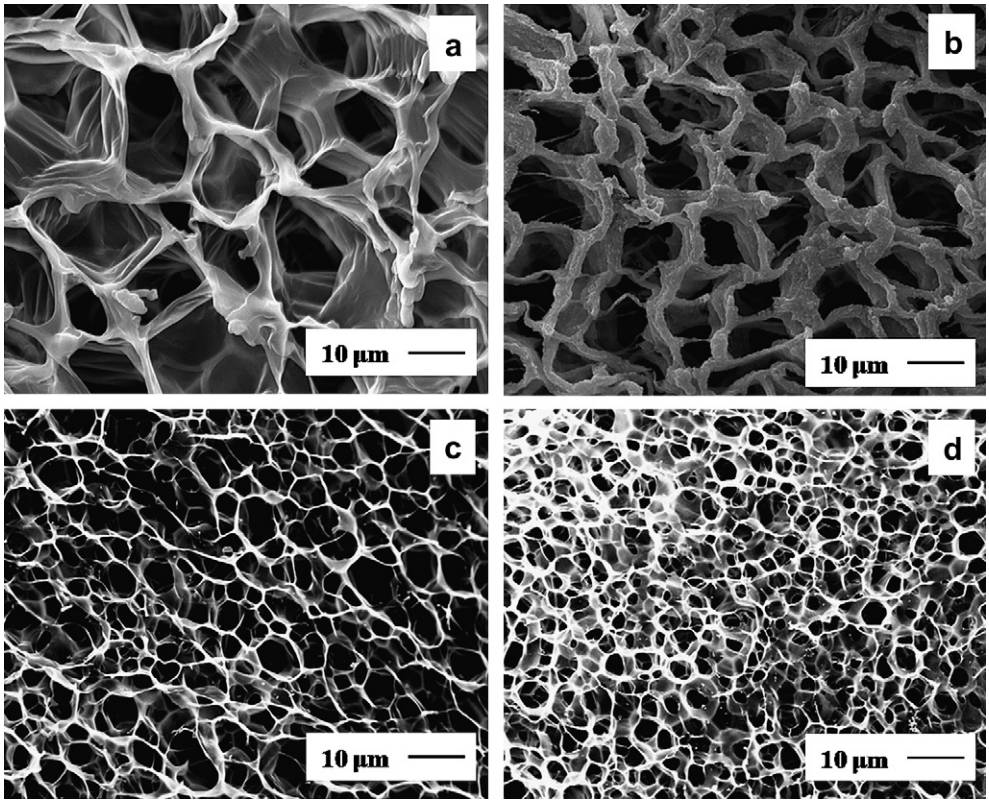

Fig. 7. SEM images of PEA-AG-G_{PEG} hydrogels. a: pure PEG-DA hydrogel; b: 8-Phe-4-AG-4-25-G_{PEG}; c: 8-Phe-4-AG-4-33-G_{PEG}; d: 8-Phe-4-AG-4-50-G_{PEG}.

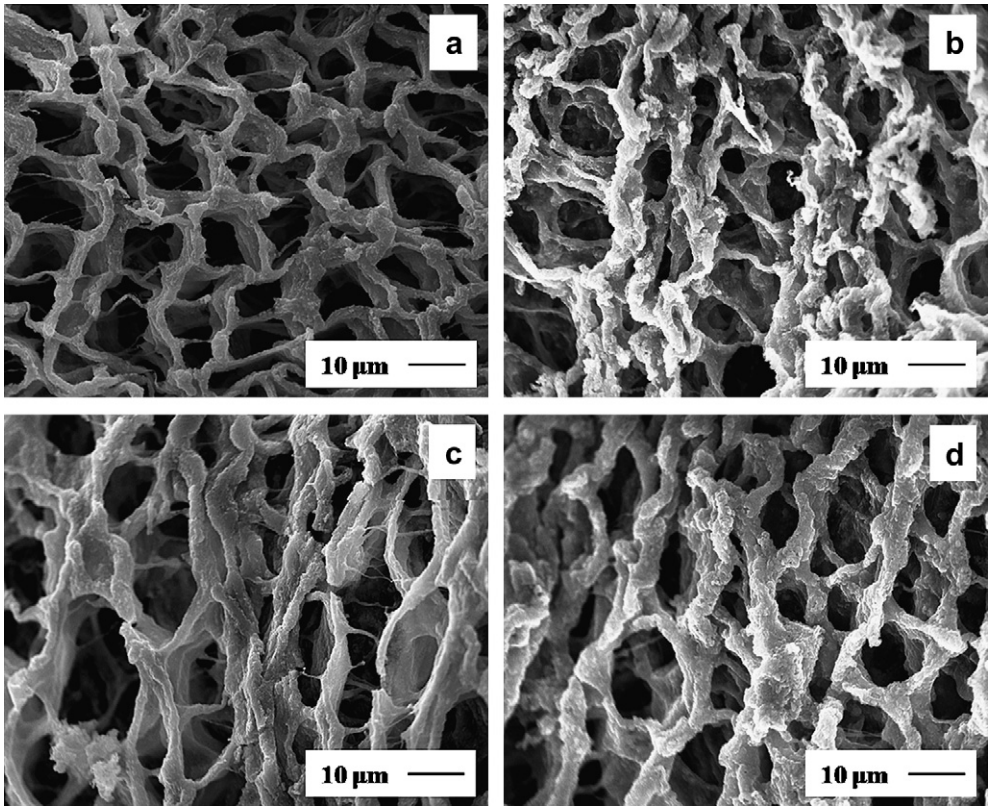

Fig. 8. Effect of the methylene chain length (x, y and z in the x-Phe-y-AG-z) of PEA-AG precursors on the PEA-AG-G_{PEG} interior morphological structures. a: 8-Phe-4-AG-4-25-G_{PEG}; b: 2-Phe-4-AG-4-25-G_{PEG}; c: 8-Phe-6-AG-4-25-G_{PEG}; d: 8-Phe-4-AG-6-25-G_{PEG}.

All these methylene chain length change had little effects on the interior morphology of PEA-AG-G_{PEG} hydrogels even though the PEA-AG precursors had different double bond density.

Comparing with the UPEA-based hydrogels [20], the hydrogels from PEA-AG had relatively larger pores than those with double bonds in the diamide portion in UPEA backbone, as the pore size of hydrogels formed from 2-Phe-4-AG-4-50-G_{PEG} precursor was 7.2 ± 2.0 μm, while UPEA 2-UPhe-4 was less than 5 μm. It was consistent with the equilibrium swelling data Q_{eq} and mechanical data that the reactivity of the pendant double bonds in PEA-AG was lower than those double bonds in the diamide portion in UPEA backbone; as a result, a looser network structure of larger pore size would be formed when photocrosslinking with PEG-DA.

3.4.2. PEA-AG/Pluronic-DA hybrid hydrogels (PEA-AG-$G_{Pluronic}$)

Fig. 9 showed the SEM images of the PEA-AG/Pluronic-DA hybrid hydrogels PEA-AG-$G_{Pluronic}$ (Fig. 9b–d) and the pure Pluronic-DA hydrogel (Fig. 9a). Like the prior PEA-AG-G_{PEG} hybrid hydrogel system, the PEA-AG-$G_{Pluronic}$ hybrid hydrogels had smaller pore size than the pure Pluronic-DA hydrogel, and the similar trend of the AG content in the PEA-AG precursor on the pore size as the PEA-AG-G_{PEG} system was observed. For example, the pore size of pure Pluronic-DA hydrogel was about 21.8 ± 5.5 μm, while 8-Phe-4-AG-4-25-$G_{Pluronic}$ had the pore size of 14.6 ± 3.4 μm. As the AG contents in the PEA-AG precursor increased, the resulting PEA-AG-$G_{Pluronic}$ hybrid hydrogels showed smaller pore size. The pore size of the 8-Phe-4-AG-4-33-$G_{Pluronic}$ was reduced to 10.5 ± 2.6 μm, and the pore size was reduced further to 6.2 ± 2.7 μm in the 8-Phe-4-AG-4-50-$G_{Pluronic}$.

This reduction in pore size of the hybrid hydrogels of both the PEA-AG-G_{PEG} and PEA-AG-$G_{Pluronic}$ systems with an increase in the AG contents in the PEA-AG precursor was consistent with the observed DMA and equilibrium swelling data described previously. An increase in the AG contents in the PEA-AG precursor, more double bonds in the PEA-AG precursor could become available for the subsequent photocrosslinking gelation. As a result, a tighter network structure of smaller pore size would be formed with lower equilibrium swelling but higher compressive moduli as observed (Table 2).

Comparing with the corresponding PEA-AG-G_{PEG} hydrogel (for example, 8-Phe-4-AG-4-25-G_{PEG} vs. 8-Phe-4-AG-4-25-$G_{Pluronic}$), the PEA-AG-$G_{Pluronic}$ hydrogel had relatively larger pore size and thicker wall. When Pluronic-DA photo-crosslinked with the corresponding PEA-AG precursor, the hydrogels formed would have a relatively looser network structure due to the lower double bond density in Pluronic-DA precursor. This was also consistent with the observed DMA and equilibrium swelling data in Table 2 that PEA-AG-$G_{Pluronic}$ hydrogel had higher equilibrium swelling ratio and lower compressive moduli than the corresponding PEA-AG-G_{PEG} hydrogel.

3.5. Short-term in vitro biodegradation of PEA-AG/PEG-DA hybrid hydrogels PEA-AG-G_{PEG}

The short-term *in vitro* biodegradation property of the PEA-AG/PEG-DA hybrid hydrogels PEA-AG-G_{PEG} were investigated in both PBS buffer and α-chymotrypsin solutions of pH 7.4 at 37 °C. The biodegradability of 8-Phe-4-AG-4-G_{PEG} was evaluated by the weight loss over 30 days. The biodegradation data of 8-Phe-4-AG-4-G_{PEG} were showed in Figs. 10 and 11.

The biodegradation rate of 8-Phe-4-AG-4-25-G_{PEG} in the α-chymotrypsin solution was faster than in pure PBS buffer, and the

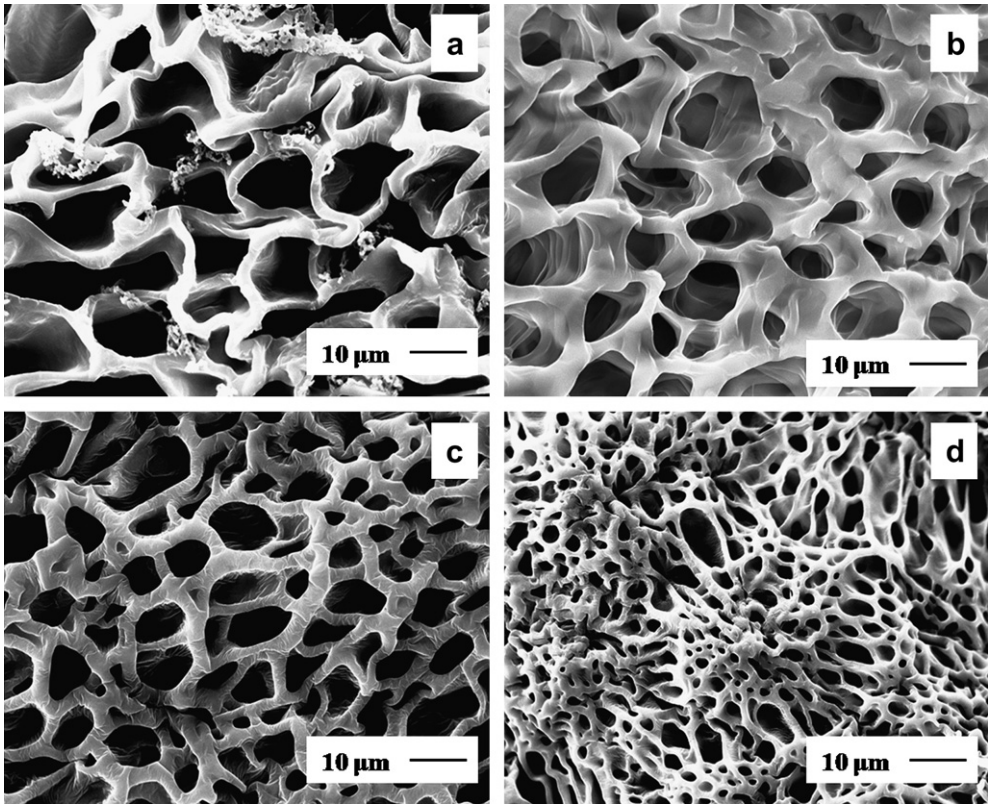

Fig. 9. SEM images of PEA-AG-$G_{Pluronic}$ hydrogels. a: pure Pluronic-DA hydrogel; b: 8-Phe-4-AG-4-25-$G_{Pluronic}$; c: 8-Phe-4-AG-4-33-$G_{Pluronic}$; d: 8-Phe-4-AG-4-50-$G_{Pluronic}$.

biodegradation rate increased with an increase in the α-chymotrypsin concentration as shown in Fig. 10. In the 30 days incubation period, the 8-Phe-4-AG-4-25-G_{PEG} sample had a 23 ± 1% weight loss in pure PBS buffer, while the weight loss increased to 42 ± 2% and 55 ± 3% in 0.1 and 0.2 mg/mL α-chymotrypsin solutions, respectively.

The biodegradation rate increased with an increase in the allylglycine (AG) content in the PEA-AG precursor (Fig. 11). The 8-Phe-4-AG-4-50-G_{PEG} sample had a 70 ± 4% weight loss when comparing with the 55 ± 3% weight loss of the 8-Phe-4-AG-4-25-G_{PEG} sample in the 30 days incubation in the 0.2 mg/mL α-chymotrypsin solution. As the Phe-4 to AG-4 feed ratio decreased (AG increased), the pendant double bonds located in the AG unit increased, consequently, more crosslinkable sites became available to form tighter network structure (i.e., more mass per volume), therefore the hydrogel formed was more hydrophobic, which would be more affinitive to α-chymotrypsin. This increase in biodegradation rate of the PEA-AG-G_{PEG} hydrogels with an increase in the AG contents in the PEA-AG precursor was consistent with the observed DMA and equilibrium swelling data described previously. An increase in the

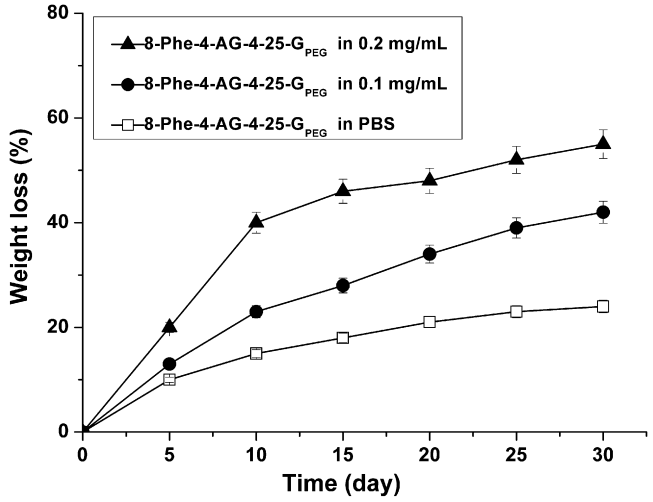

Fig. 10. Biodegradation behaviors of 8-Phe-4-AG-4-25-G_{PEG} in different α-chymotrypsin concentration.

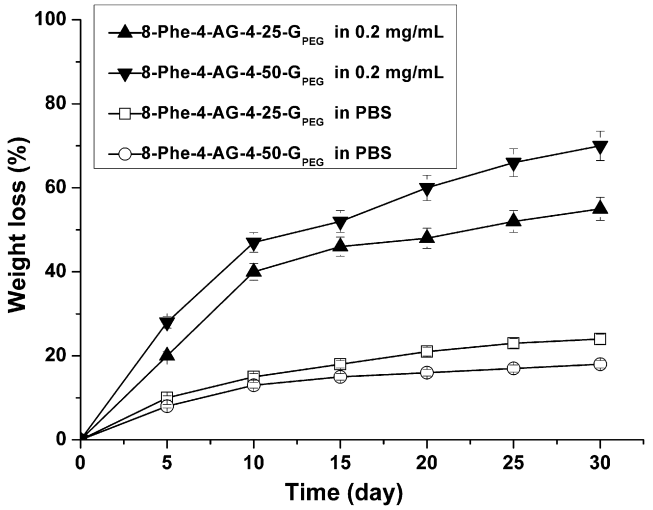

Fig. 11. Biodegradation behaviors of 8-Phe-4-AG-4-G_{PEG} with different allylglycine segment content in 0.2 mg/mL α-chymotrypsin solution and pure PBS.

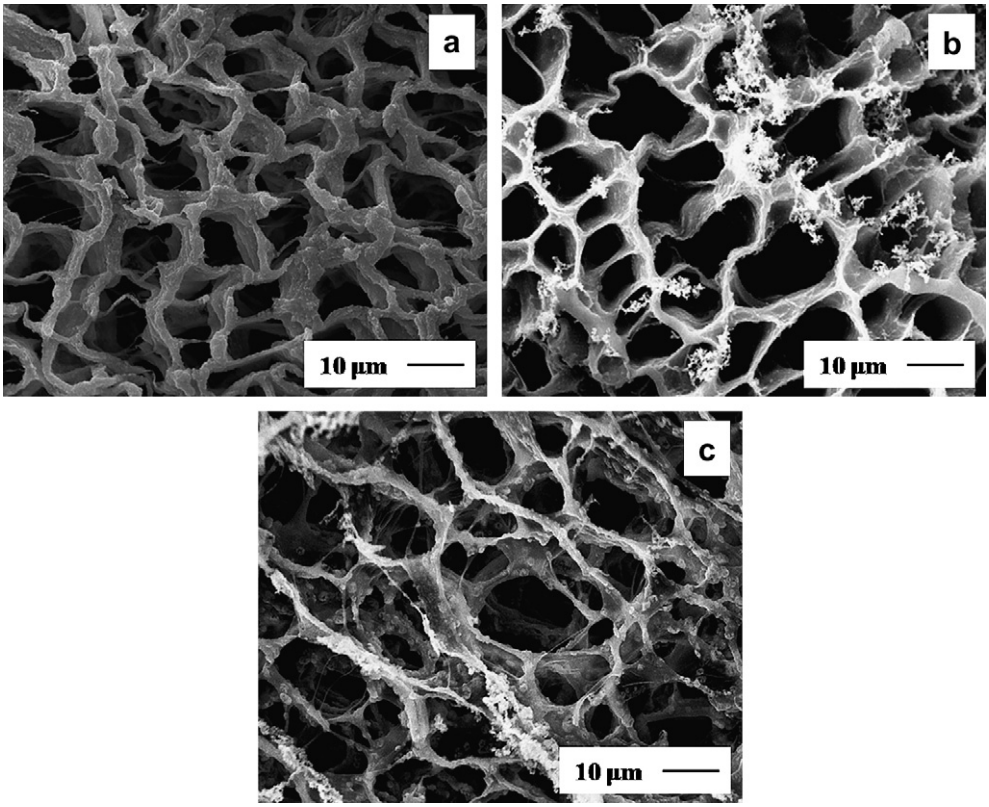

Fig. 12. SEM images of 8-Phe-4-AG-4-25-G_{PEG} in 0.2 mg/mL α-chymotrypsin solution. a: day 0; b: day 15; c: day 30.

AG contents in the PEA-AG precursor, more double bonds in the PEA-AG precursor could become available for the subsequent photo-crosslinking gelation. As a result, a tighter network structure would be formed with lower equilibrium swelling but higher compressive moduli as observed (Table 2). However, the biodegradation rate of the PEA-AG-G_{PEG} in a pure PBS buffer decreased with an increase in the AG content in the PEA-AG precursor, for example, the 8-Phe-4-AG-4-50-G_{PEG} sample had only 18 ± 1% weight loss when comparing with the 23 ± 1% weight loss of the 8-Phe-4-AG-4-25-G_{PEG} sample in the 30 days incubation. In a pure PBS buffer, both 8-Phe-4-AG-4-50-G_{PEG} and 8-Phe-4-AG-4-25-G_{PEG} had relatively higher weight loss compared with 8-Phe-4-AG-4 polymer. That could be attributed to the loss of PEG component which became partially dissolved during the incubation.

Comparing with the UPEA-based hydrogels [17], the PEA-AG-G_{PEG} hydrogels had slightly lower biodegradation rate than those UPEAs with double bond in the diamide portion. For example, after 30-day incubation, hydrogels formed from UPEA precursor (2-UPhe-4) had 63 ± 5% weight loss, while 8-Phe-4-AG-4-25-G_{PEG} had 55 ± 3% weight loss under the same conditions (in 0.2 mg/mL α-chymotrypsin solution at 37 °C). This was mainly because the UPEA-based hydrogels with double bond in the diamide portion had tighter network structure than PEA-AG based hydrogels, therefore the hydrogel formed was more hydrophobic, which would be more affinitive to α-chymotrypsin.

The interior morphology changes of the PEA-AG-G_{PEG} upon biodegradation were shown in Figs. 12–14. The interior morphology of 8-Phe-4-AG-4-25-G_{PEG} incubated in 0.2 mg/mL α-chymotrypsin solution at day 0, 15 and 30 were shown in Fig. 12. With the increasing incubation time (Fig. 12a–c), the network gradually became looser and pore size became larger. Similar result was found for 8-Phe-4-AG-4-50-G_{PEG} (Fig. 13). The interior morphology of 8-Phe-4-AG-4-25-G_{PEG} incubated in a pure PBS buffer at day 0 and 30 was shown in Fig. 14. The morphology

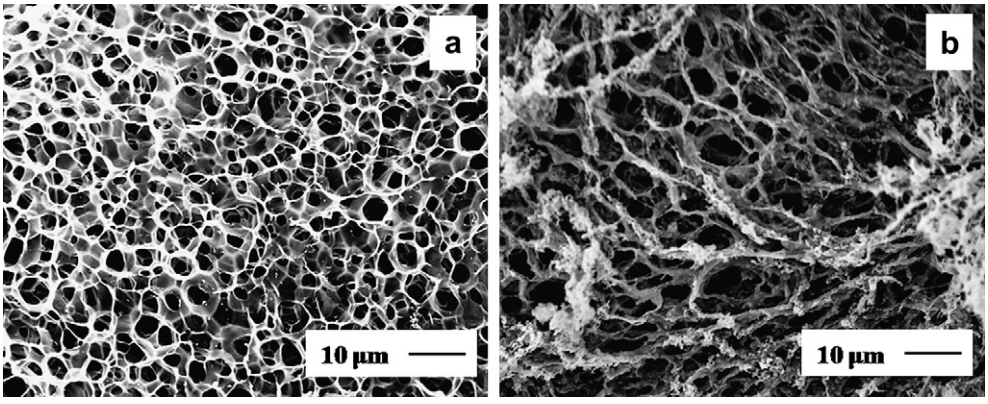

Fig. 13. SEM images of 8-Phe-4-AG-4-50-G_{PEG} in 0.2 mg/mL α-chymotrypsin solution. a: day 0; b: day 30.

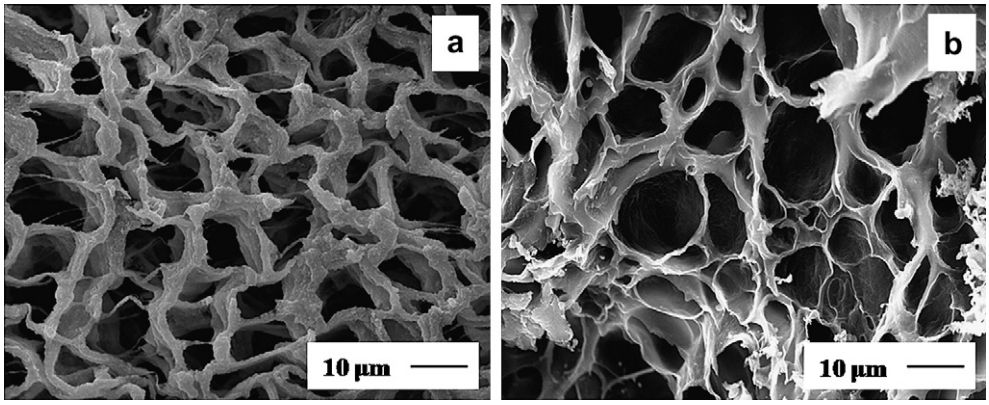

Fig. 14. SEM images of 8-Phe-4-AG-4-25-G_{PEG} in pure PBS buffer. a: day 0; b: day 30.

changes in PBS buffer were not as obvious as in α-chymotrypsin solution, although there still had some weight loss. This was also in agreement with the previous weight loss data that 8-Phe-4-AG-4-25-G_{PEG} had only about a 23 ± 1% weight loss after 30-day incubation in pure PBS buffer.

4. Conclusions

A series of novel biodegradable hydrogels were designed and fabricated from a new functional poly(ester amide) precursor and poly(ethylene glycol) diacrylate and Pluronic diacrylate co-precursors by UV photocrosslinking means. These new hybrid hydrogels were characterized for interior morphology, equilibrium swelling ratio (Q_{eq}), and compression modulus. All these hybrid hydrogels showed three-dimensional porous structures and their pore size of the hydrogels reduced with an increase in the AG contents (i.e., double bond contents) in the PEA-AG precursor. The short-term *in vitro* biodegradation processes of PEA/PEG-DA hybrid hydrogels PEA-AG-G_{PEG} were investigated in both PBS buffer and α-chymotrypsin solutions. The biodegradation rate of PEA-AG-G_{PEG} in α-chymotrypsin solution was faster than in pure PBS buffer. And the biodegradation rate increased with the increase of α-chymotrypsin concentration.

Acknowledgment

The partial support of the Cornell University Morgan Tissue Engineering Seed Grant Program is greatly appreciated.

References

[1] Inoue T, Chen G, Nakamae K, Hoffman AS. A hydrophobically-modified bioadhesive polyelectrolyte hydrogel for drug delivery. J Control Release 1997;49(2(3)):167–76.
[2] Uhrich KE, Cannizzaro SM, Langer RS, Shakesheff KM. Polymeric systems for controlled drug release. Chem Rev 1999;99(11):3181–98.
[3] Albertsson A-C, Varma IK. Recent developments in ring opening polymerization of lactones for biomedical applications. Biomacromolecules 2003;4(6):1466–86.
[4] Chiellini E, Solaro R. Biodegradable polymeric materials. Adv Mater 1996;8(4):305–13.
[5] Drumright RE, Gruber PR, Henton DE. Polylactic acid technology. Adv Mater 2000;12(23):1841–6.
[6] Eguiburu JL, Fernandez-Berridi MJ, Cossio FP, San Roman J. Ring-opening polymerization of L-lactide initiated by (2-methacryloxy)ethyloxy-aluminum trialkoxides. 1. Kinetics. Macromolecules 1999;32(25):8252–8.
[7] Mooney DJ, Organ G, Vacanti JP, Langer R. Design and fabrication of biodegradable polymer devices to engineer tubular tissues. Cell Transplant 1994;3(2):203–10.
[8] O'Keefe BJ, Breyfogle LE, Hillmyer MA, Tolman WB. Mechanistic comparison of cyclic ester polymerizations by novel iron(III)-alkoxide complexes: single vs multiple site catalysis. J Am Chem Soc 2002;124(16):4384–93.
[9] O'Keefe BJ, Hillmyer MA, Tolman WB. Polymerization of lactide and related cyclic esters by discrete metal complexes. J Chem Soc Dalton Trans 2001;15:2215–24.
[10] Takeuchi D, Nakamura T, Aida T. Bulky titanium bis(phenolate) complexes as novel initiators for living anionic polymerization of e-caprolactone. Macromolecules 2000;33(3):725–9.
[11] Zhong Z, Dijkstra PJ, Birg C, Westerhausen M, Feijen J. A novel and versatile calcium-based initiator system for the ring-opening polymerization of cyclic esters. Macromolecules 2001;34(12):3863–8.
[12] Lee Seung H, Szinai I, Carpenter K, Katsarava R, Jokhadze G, Chu C-C, et al. In-vivo biocompatibility evaluation of stents coated with a new biodegradable elastomeric and functional polymer. Coron Artery Dis 2002;13(4):237–41.
[13] Guo K, Chu CC, Chkhaidze E, Katsarava R. Synthesis and characterization of novel biodegradable unsaturated poly(ester amide)s. J Polym Sci A Polym Chem 2005;43(7):1463–77.
[14] Li L, Chu C- C. Nitroxyl radical incorporated electrospun biodegradable poly(ester amide) nanofiber membranes. J Biomater Sci Polym Ed 2009;20(3):341–61.
[15] Guo K, Chu CC. Copolymers of unsaturated and saturated poly(ether ester amide)s: synthesis, characterization, and biodegradation. J Appl Polym Sci 2008;110(3):1858–69.
[16] Guo K, Chu CC. Synthesis, characterization, and biodegradation of novel poly (ether ester amide)s based on L-phenylalanine and oligoethylene glycol. Biomacromolecules 2007;8(9):2851–61.
[17] Guo K, Chu CC. Biodegradation of unsaturated poly(ester-amide)s and their hydrogels. Biomaterials 2007;28(22):3284–94.
[18] Guo K, Chu CC. Synthesis, characterization, and biodegradation of copolymers of unsaturated and saturated poly(ester amide)s. J Polym Sci A Polym Chem 2007;45(9):1595–606.
[19] Jokhadze G, Machaidze M, Panosyan H, Chu CC, Katsarava R. Synthesis and characterization of functional elastomeric poly(ester amide) co-polymers. J Biomater Sci Polym Ed 2007;18(4):411–38.
[20] Guo K, Chu CC. Synthesis and characterization of novel biodegradable unsaturated poly(ester amide)/poly(ethylene glycol) diacrylate hydrogels. J Polym Sci A Polym Chem 2005;43(17):3932–44.
[21] Tsitlanadze G, Kviria T, Katsarava R, Chu CC. In vitro enzymatic biodegradation of amino acid based poly(ester amide)s biomaterials. J Mater Sci Mater Med; 2004:185–90.
[22] Tsitlanadze G, Machaidze M, Kviria T, Djavakhishvili N, Chu CC, Katsarava R. Biodegradation of amino-acid-based poly(ester amide)s: in vitro weight loss and preliminary in vivo studies. J Biomater Sci Polym Ed 2004;15(1):1–24.
[23] Katsarava R, Beridze V, Arabuli N, Kharadze D, Chu CC, Won CY. Amino acid-based bioanalogous polymers. synthesis, and study of regular poly(ester amide)s based on bis(alpha -amino acid) alpha, w-alkylene diesters, and aliphatic dicarboxylic acids. J Polym Sci A Polym Chem 1999;37(4):391–407.
[24] Schwartz Suzanne, Demars S, Chu CC, White J, Cooper A, Rothrock M, et al. Efficacy of poly(ester amide) dressings on partial thickness wound healing. Toronto, Canada: 3rd World Union of Wound Healing Societies, June 4-8, 2008; 2008.
[25] De Fife KM, Grako K, Cruz-Aranda G, Price S, Chantung R, MacPherson K, et al. Poly(ester amide) co-polymers promote blood and tissue compatibility. J Biomater Sci Polym Ed 2009;20(11):1495–511.
[26] Garg P, Keul H, Klee D, Moeller M. Concept and synthesis of poly(ester amide)s with one isolated, two or three consecutive amide bonds randomly distributed along the polyester backbone. Des Monomers Polym 2009;12(5):405–24.
[27] Guo K, Chu CC. Biodegradable and injectable paclitaxel-loaded poly(ester amide)s microspheres: fabrication and characterization. J Biomed Mater Res B Appl Biomater 2009;89B(2):491–500.
[28] Chu CC, Sun Dajun D. New electrospun synthetic biodegradable poly(ester amide) drug-eluting fibrous membranes for potential wound treatment. In: AATCC Symposium Proceeding "Medical, Nonwovens, and Technical Textiles" 2008 Oct. 6-7. Durham, NC; 2008. p. 60–76.

[29] Guo K, Chu CC. Controlled release of paclitaxel from biodegradable unsaturated poly(ester amide)s/poly(ethylene glycol) diacrylate hydrogels. J Biomater Sci Polym Ed 2007;18(5):489–504.
[30] Yamanouchi D, Wu J, Lazar AN, Craig Kent K, Chu C-C, Liu B. Biodegradable arginine-based poly(ester-amide)s as non-viral gene delivery reagents. Biomaterials 2008;29(22):3269–77.
[31] Pang X, Chu CC. Synthesis, characterization and biodegradation of functionalized amino acid-based poly(ester amide)s. Biomaterials 2010;31(14):3745–54.
[32] Song H. L-Arginine based biodegradable poly(ester amide)s, their synthesis, characterization, fabrications, and applications as drug and gene carriers. PhD thesis: Cornell University; 2007.